HHS Public Access

Author manuscript

Biomaterials. Author manuscript; available in PMC 2017 January 01.

Published in final edited form as:

Biomaterials. 2016 January ; 77: 164–172. doi:10.1016/j.biomaterials.2015.10.059.

A 3D in vitro model of patient-derived prostate cancer xenograft for controlled interrogation of in vivo tumor-stromal interactions

Eliza L. S. Fong[1], **Xinhai Wan**[2], **Jun Yang**[2], **Micaela Morgado**[3], **Antonios G. Mikos**[1], **Daniel A. Harrington**[3], **Nora M. Navone**[2,*], and **Mary C. Farach-Carson**[1,2,3,*]

[1]Department of Bioengineering, Rice University, 6500 Main Street, Houston, TX 77030, USA

[2]Department of Genitourinary Medical Oncology and the David H. Koch Center for Applied Research of Genitourinary Cancers, The University of Texas MD Anderson Cancer Center, Houston, TX 77030, USA

[3]Department of BioSciences, Rice University, 6500 Main Street, Houston, TX 77030, USA

Abstract

Patient-derived xenograft (PDX) models better represent human cancer than traditional cell lines. However, the complex in vivo environment makes it challenging to employ PDX models to investigate tumor-stromal interactions, such as those that mediate prostate cancer (PCa) bone metastasis. Thus, we engineered a defined three-dimensional (3D) hydrogel system capable of supporting the co-culture of PCa PDX cells and osteoblastic cells to recapitulate the PCa-osteoblast unit within the bone metastatic microenvironment in vitro. Our 3D model not only maintained cell viability but also preserved the typical osteogenic phenotype of PCa PDX cells. Additionally, co-culture cellularity was maintained over that of either cell type cultured alone, suggesting that the PCa-osteoblast cross-talk supports PCa progression in bone, as is hypothesized to occur in patients with prostatic bone metastasis. Strikingly, osteoblastic cells co-cultured with PCa PDX tumoroids organized around the tumoroids, closely mimicking the architecture of PCa metastases in bone. Finally, tumor-stromal signaling mediated by the fibroblast growth factor axis tightly paralleled that in the in vivo counterpart. Together, these findings indicate that this 3D PCa PDX model recapitulates important pathological properties of PCa bone metastasis, and validate the use of this model for controlled and systematic interrogation of complex in vivo tumor-stromal interactions.

[*]To whom correspondence should be addressed: Mary C. Farach-Carson, Department of BioSciences, Rice University, 6500 Main Street, Houston, TX 77030, USA, farachca@rice.edu, Phone: +1 (713) 348 5052 or Nora M. Navone, Department of Genitourinary Medical Oncology and David H. Koch Center for Applied Research of Genitourinary Cancers, The University of Texas MD Anderson Cancer Center, 1515 Holcombe Blvd., Houston, TX 77030, USA, nnavone@mdanderson.org.

Conflict of Interest: All authors confirm that there are no conflicting interests.

Keywords

Patient-derived xenograft; prostate cancer; three-dimensional; co-culture; osteoblasts; hydrogel; model

Introduction

Given the heavy investment in understanding cancer over the past several decades, the high drug attrition rates in oncologic drug development are disappointing (1). The poor translation of seemingly promising preclinical findings to clinical success is partly due to the heavy reliance on cancer cell lines as tumor models for preclinical studies (2). Recently, patient-derived xenograft (PDX) models have emerged as better surrogates of human cancer. PDX models, developed through serial propagation of patient tumor tissue in murine hosts, closely resemble the parental tumor in histology, gene expression profiles, preserved heterogeneity, and drug response (3–7). However, use of PDX models in in vitro mechanistic studies is hampered by their poor adaptation to traditional two-dimensional tissue culture and the potential for two-dimensional culture to induce undesired adaptations (6,8). Improved methods for in vitro PDX culture have been developed that rely on three-dimensional (3D) cell culture strategies, such as spheroid culture, or encapsulation of tumor cells within naturally derived gels such as Matrigel or collagen (9–12). However, while spheroid cultures enable primary tumor tissue culture, the lack of a surrounding matrix prohibits control over spatial positioning of multiple cell types. Similarly, the often ill-defined and variable composition of naturally derived gels makes consistent re-creation of the engineered in vitro tumor microenvironment challenging.

In current paradigms, cancer is viewed as a complex manifestation of aberrant interactions between tumor cells and the surrounding stromal compartment. Accordingly, increasing emphasis is being placed on understanding the role of the host cells in the tumor microenvironment in cancer progression and metastasis and in design of therapies (13). In prostate cancer (PCa), stromal-epithelial signaling dictates tumor cell behavior and metastasis (14–16). Metastasizing PCa cells predominantly target bone, and the characteristic osteoblastic lesions that form reflect the functional dependency of PCa on the bone microenvironment for disease progression. Therefore, targeting the bone stroma and disrupting the PCa-stromal cross-talk can be an effective therapeutic strategy for treating or preventing bone metastases (17). In our recent integrated clinical and preclinical studies using the MDA PCa 118b PDX model, we demonstrated that blockade of fibroblast growth factor receptor (FGFR)-dependent PCa-stromal interactions in the bone microenvironment could be an effective therapeutic strategy for a subset of PCa patients (17). In light of these findings, we wished to further investigate the specific stromal targets and affected pathways to guide biomarker development and patient selection. However, in vitro platforms to support such mechanistic studies of PCa PDX-stromal interactions had to be created.

In the interdisciplinary study reported here, we addressed this need by developing and validating an in vitro PCa PDX model that accurately reflects PCa-stromal interactions in bone for controlled mechanistic studies. We demonstrate for the first time, to our

knowledge, an engineered tumor microenvironment consisting of clinically relevant PDX tumor cells and osteoblastic cells, co-encapsulated within a well-defined 3D hyaluronan (HA) hydrogel. Osteoblasts play a key role in promoting PCa progression in bone (18). Ubiquitous in the extracellular matrix of connective tissues, HA is a building block for the fabrication of hydrogel matrices designed to mimic HA-rich tissues such as the bone marrow, where bone metastatic PCa cells reside (19,20). Indeed, we previously reported the first demonstration of using a 3D scaffold-based approach to culture PDX cells in vitro in unmodified HA hydrogels (21). Prior to development of our 3D hydrogel approach, it was difficult to culture PCa PDX cells in vitro for experimentation given their poor viability on tissue culture plastic. In this work, to enable the culture of osteoblastic cells with PCa PDX cells, HA was specifically modified with integrinbinding peptides and cross-linked with matrix metalloproteinase (MMP)-degradable peptides. Plain, unmodified HA hydrogels are not capable of supporting the attachment and spreading of encapsulated osteoblastic cells. Incorporation of these peptides is an approach that was previously developed to enable cell-mediated remodeling of synthetic 3D hydrogels for tissue regeneration applications (22–24). This PDX co-culture model maintains key phenotypic tumor markers; recapitulates the in vivo structural arrangement of osteoblasts with respect to tumor cells; mimics many elements of the previously observed FGFR-mediated tumor-stromal crosstalk for PDX tumor cells grown in bone, including cross-talk involving FGFR1 and fibroblast growth factor 9 (FGF9) (17,25); and offers a robust platform for in vitro drug evaluation. This model addresses the critical unmet need in PCa research and drug discovery for platforms that support the controlled interrogation of complex in vivo tumor-stromal interactions as discrete units in vitro.

Materials and Methods

Study design

The primary objective of this study was to develop an auxiliary model to the in vivo PCa PDX model that supports controlled mechanistic studies of tumor-stromal interactions in vitro. We cultured PCa PDX cells and osteoblastic cells within a well-defined 3D hydrogel matrix and characterized the tumor architecture, viability, phenotype, as well as the biochemical interaction between the two cell populations. These findings were then validated against the corresponding PCa PDX in vivo model (17). We also evaluated whether (1) standard molecular biology tools (such as gene knockdown) can be employed to manipulate cell-cell interactions for mechanistic investigations and (2) the effect of dovitinib in vivo (17) can be at least in part, reflected in this in vitro PCa PDX model.

Synthesis and characterization of thiolated HA

Sulfhydryl groups were incorporated in HA (620 kDa, Genzyme, Cambridge, MA) by reacting HA with a disulfide-containing dihydrazide compound, followed by reduction with dithiothreitol, using a previously reported method (20,26). The degree of modification (35–43%) in thiolated HA was measured (20,26) by ^{1}H nuclear magnetic resonance, and the lyophilized product was stored at −20°C under argon prior to use.

Synthesis of acrylated peptides

Cell-adhesive peptide GRGDS (GenScript USA Inc., Piscataway, NJ) with C-terminal amidation was reacted with acrylate-PEG-SVA (3400 g/mol, Laysan Bio Inc., Arab, AL) at a molar ratio of 1.2:1 in HEPBS buffer (20 mM HEPBS [Santa Cruz Biotechnology, Inc., Dallas, TX], 100 mM NaCl, 2 mM $CaCl_2$, and 2 mM $MgCl_2$) adjusted to pH 8.0 using 0.1N NaOH (27). The reaction was allowed to run overnight at 4°C on a shaker pro tected from light and then dialyzed for 2 days against ultrapure water using a 3500-Da MWCO dialysis membrane (Spectrum Laboratories Inc., Rancho Dominguez, CA) before lyophilization for an additional 2 days. MMP-degradable peptide, KGGGPQG↓IWGQGK (GenScript USA Inc.) with N-terminal acetylation, herein referred to as PQ (↓ marks the MMP-cleavable site), was reacted with acrylate-PEG-SVA at a molar ratio of 1:2.5 using the same protocol. Conjugation of acrylate-PEG to the peptides was verified by high-performance liquid chromatography (Vydak C_{18} 218TP54 column, Varian Prostar solvent delivery module and UV-vis detector) and MALDI-TOF (Bruker AutoFlex II). The lyophilized solids were stored at −20°C prior to use.

MDA PCa 118b PCa PDX in vivo propagation and processing

The MDA PCa 118b PDX (25) was routinely maintained as subcutaneous tumors in CB-17 SCID mice (Charles River). Propagation of tumors in mice was conducted under approval by the Institutional Animal Care and Use Committee of The University of Texas MD Anderson Cancer Center. Following harvest, the tumors were processed for hydrogel encapsulation as previously described (21). To obtain sections of MDA PCa 118b PDX in bone for histologic characterization, tumor-bearing femurs were prepared and processed as previously described (25).

Cell culture

MC 3T3-E1 (ATCC, Manassas, VA) cells were maintained in alpha-MEM (Life Technologies, Grand Island, NY) containing 10% (v/v) FBS and in the presence of 100 U/mL penicillin and 100 μg/mL streptomycin at 37°C and 5% CO_2.

Preparation of cell-laden hydrogel constructs

To prepare the MDA PCa 118b-only constructs, following our previously established protocol (21), tumor cell aggregates that formed in suspension were mixed with thiolated HA dissolved in PBS to 10 mg/mL. Each MDA PCa 118b-only construct was prepared with a theoretical encapsulation density of 300,000 cells (21). Next, acrylate-PEG-GRGDS (73.7 mg/mL) and acrylate-PEG-PQ-PEG-acrylate (37.0 mg/mL) dissolved in PBS were added to the mixture at a volume ratio of 4:1:1 (thiolated SH: acrylate-PEG-GRGDS: acrylate-PEG-PQ-PEG-acrylate). Final concentrations of GRGDS and PQ in each resulting 42-μL hydrogel construct were 3 mM and 0.73 mM, respectively. The tumor cell–hydrogel mixture was then pipetted into custom-made PDMS molds as previously described (21) and allowed to cross-link for 1 h before immersion in cell culture medium and incubation overnight. Cell-laden hydrogel constructs were transferred into 12-well plates the next day. Medium was exchanged every 2 days. MC 3T3-E1 mono-culture constructs were prepared in a similar manner with encapsulation density of 100,000 cells per construct. To prepare the co-

culture constructs, a theoretical encapsulation density of 300,000 tumor cells and actual density of 100,000 MC 3T3-E1 cells per hydrogel construct was used. A 1:1 (v/v) mixture of DMEM/F-12 and alpha-MEM medium supplemented with 2% (v/v) FBS was used for all studies.

Immunocytochemistry

As described previously (21), cell-hydrogel constructs in 12-well plates were washed with PBS, fixed with 4% (v/v) paraformaldehyde for 10 min at room temperature, and processed for immunostaining as described in Supplementary Materials.

Cell viability and growth

Cell viability was evaluated using the LIVE/DEAD viability/cytotoxicity kit (Life Technologies) per the manufacturer's instructions. At the designated time point, cell-hydrogel constructs were incubated in 400 μL of 2 μM calcein-AM and 4 μM ethidium homodimer in PBS for 40 min at 37°C on a shaker before confocal imaging. To assess growth, the Quant-iT PicoGreen dsDNA quantification assay (Life Technologies) was used per the manufacturer's instructions as described in Supplementary Materials.

Quantitative PCR

At the designated time point, cell-hydrogel constructs were collected into microcentrifuge tubes. Then 500 μL of Trizol (Life Technologies) was added, and an 18-gauge needle and 1-mL syringe were used to mechanically dissociate the hydrogel constructs. Samples were then stored at −80°C and processed for RNA isolation, cD NA synthesis, and real-time PCR per the manufacturers' instructions (Supplementary Materials).

Dovitinib studies

MDA PCa 118b-only, MC 3T3-E1-only, and co-culture constructs were prepared and cultured for 4 days. Dovitinib (Novartis, Pharma AG) was dissolved in fresh medium (0, 500, or 1000 nM) and added to the constructs. Cells were incubated in dovitinib-containing medium for an additional 4 days with one medium change. At the designated time point, constructs were collected and stored at −80°C before the dsDNA quantification assay was run or processed for RNA isolation. DNA content was quantified in a repeat experiment under identical conditions. Within each study, measured DNA contents from each group (n = 4) were normalized against the average DNA content of the MC 3T3-E1-only untreated group, and values from the two studies were combined (n = 8) and averaged.

Fgfr1-knockdown MC 3T3-E1 studies

Fgfr1-knockdown MC 3T3-E1 cells and the corresponding controls were prepared using the ON-TARGETplus Mouse Fgfr1 (14182) siRNA–SMARTpool and ON-TARGETplus nontargeting Pool (GE Dharmacon, Lafayette, CO) in the presence of HiPerFect transfection reagent (Qiagen, Valencia, CA) according to the manufacturers' protocols. MC 3T3-E1 cells were incubated with 30 nM of siRNA and the HiPerFect transfection reagent for 3 days before hydrogel encapsulation either alone or with the MDA PCa 118b cells. At each

designated time point, constructs were collected and stored at −80°C before the dsDNA quantification assay was run or processed for RNA isolation.

Statistical methods

Data are expressed as mean ± standard deviation. Differences between paired data were tested using Student's t test. For the dovitinib study (measured DNA content), one-way ANOVA and then Student's t test were used. For the *Fgfr1*-knockdown MC 3T3-E1 study (measured DNA content), ANOVA was performed at each time point to investigate whether cellularity differed between *Fgfr1*-knockdown MC 3T3-E1 cells and scrambled controls and between *Fgfr1*-knockdown MC 3T3-E1 cells and scrambled controls co-cultured with MDA PCa 118b cells. Differences were considered significant at $p < 0.05$.

Results

PDX-derived PCa cells and osteoblastic cells co-encapsulated in 3D hydrogel mimic in vivo tumor organization

With the goal of modeling the PCa cell-osteoblast interaction in vitro, we co-encapsulated MDA PCa 118b PDX-derived PCa tumoroids with MC 3T3-E1 osteoblastic cells within an engineered 3D hydrogel containing integrin-binding and MMP-degradable peptide sequences (Fig. 1). MDA PCa 118b is a PCa xenograft model that we previously established from bone metastases in a patient with castration-resistant PCa (25). The use of mouse-derived MC 3T3-E1 cells enabled the facile separation of gene expression trends from tumor and stroma in our co-culture system. In the absence of either the integrin-binding or MMP-degradable peptide, MC 3T3-E1 cells do not spread when encapsulated in hydrogels. Given the poor adherence of PDX-derived PCa cells to tissue culture plastic and their resulting tendency to form aggregates in suspension, we pre-generated tumoroids highly enriched for human PCa cells and depleted of mouse fibroblasts (21) prior to hydrogel encapsulation. Within this hydrogel matrix, the MC 3T3-E1 cells began to spread 1 day after encapsulation and remained spread through 6 days in culture, while the PCa tumoroids remained largely as compact multicellular aggregates (Fig. 2A). When MC 3T3-E1 cells were co-cultured with MDA PCa 118b tumoroids, the MC 3T3-E1 cells also began to spread 1 day after encapsulation, and these cells extended their osteoblastic processes towards and around the tumoroids over time, with this effect most evident at day 6 in culture (Fig. 2A). To better visualize this interaction, representative hydrogel constructs were immunostained for epithelial cell adhesion molecule (EpCAM) and vimentin to distinguish the epithelial tumor cells from the mesenchymal osteoblastic cells (Fig. 2, B and C). As shown in Fig. 2C, while the two cell populations were largely separate at day 1 in co-culture, progressive physical association of the MC 3T3-E1 cells and MDA PCa 118b tumoroids was observed over time, culminating in envelopment of the tumoroids by osteoblastic processes at day 6 (Fig. 2C). Quantification of the association of vimentin$^+$ cells with PCa tumoroids, in both 118b monoculture and co-culture, confirmed this rapid physical association (Fig S1). Comparison of the resulting structural organization in 3D co-culture (Fig. 2D) with the structural organization of MDA PCa 118b PDXs grown intrafemorally (Fig. 2E) indicated that our 3D co-culture model closely recapitulated the architectural arrangement of the two cell types in

vivo, i.e., a tumor mass surrounded by osteoblasts on the periphery within a mineralized matrix.

PDX-derived PCa cells co-cultured with osteoblastic cells in 3D hydrogel retain proliferative capacity

Given that MDA PCa 118b cells historically exhibit poor viability in culture (25), we next determined if our 3D hydrogel system was capable of supporting the viability of encapsulated cells over time. Both in mono-culture and in co-culture, the MDA PCa 118b and MC 3T3-E1 cells remained viable for at least 6 days in culture (Fig. 3A). To determine whether our 3D PCa co-culture model maintains tumor proliferative potential and exhibits growth characteristics necessary for drug testing, especially testing of drugs that target actively dividing cells, we evaluated the growth profile of the cultures by measuring the tumoroid size distribution over time, as well as by measuring DNA content (as an indirect indicator of cell number). Whether in mono- or co-culture, we observed an increase in tumoroid size over time (Fig. S2). Notably, the DNA content of the MDA PCa 118b-only cultures, the DNA content of the MC 3T3-E1-only cultures, and the sum of these two values were consistently lower than the DNA content of the actual co-cultures (Fig. 3B), indicating a greater-than-additive effect of the PCa cell–osteoblastic cell interaction. Further, to confirm that the tumor cells remained proliferative in our hydrogel system, we immunostained for Ki-67. Expression of Ki-67 was detected in the MDA PCa 118b cells at all time points (Fig. 3C).

PDX-derived PCa cells co-cultured with osteoblastic cells in 3D hydrogel retain the characteristics of the tumor of origin

A unique feature of MDA PCa 118b cells is their ability to trigger robust osteoblastic reactions when implanted either orthotopically in bone or ectopically as subcutaneous tumors (25). We next investigated if the PDX cells retained their osteogenic capacity when grown in our 3D hydrogels. Co-culture of MDA PCa 118b cells with MC 3T3-E1 osteoblastic cells increased transcript levels of osteoblast-enriched markers osteocalcin, bone sialoprotein, and alkaline phosphatase (ALP) in the MC 3T3-E1 cells (Fig. 3D), indicating that the MDA PCa 118b cells retained their native bone-forming phenotype. Further, we determined whether the hydrogel-encapsulated MDA PCa 118b cells expressed FGFR1 and FGF9, both of which are highly expressed by these cells in vivo (Fig. 3, E and F). Immunostaining of the hydrogel constructs for FGFR1 and FGF9 revealed that the MDA PCa 118b cells expressed both phenotypic markers in our 3D hydrogel system (Fig. 3, E and F).

PDX-derived PCa cells cultured in 3D hydrogel induce stromal Fgfr1 expression as observed in vivo

To discriminate gene expression in our human tumor–mouse osteoblast co-culture model, we used human- and mouse-specific PCR primers to probe for several signaling components in the FGF axis: *FGFR1-4*, *FGF2*, *FGF9*, and FGFR substrate 2a. MDA PCa 118b tumor cells in co-culture had gene expression similar to that of MDA PCa 118b cells in mono-culture (Fig. S3). In contrast, MC 3T3-E1 cells co-cultured with MDA PCa 118b cells had

significantly increased transcript levels of *Fgfr1* ($p = 0.001$) and *Fgfr1-IIIc* isoform ($p = 0.006$) (Fig. 4A), a finding strikingly similar to the changes seen in vivo (17). Additionally, in MC 3T3-E1 cells co-cultured with MDA PCa 118b cells, we observed a slight increase in *Fgf2* ($p = 0.057$) and decrease in *Fgfr4* ($p = 0.098$) (Fig. 4A). Expression levels of other FGF signaling components in the MC 3T3-E1 cells are shown in Fig. S4. Together, these results indicated that our 3D PCa PDX co-culture model closely recapitulates the FGFR-mediated cross-talk between PCa cells and osteoblasts in vivo.

Cross-talk between PDX-derived PCa cells and osteoblastic cells is at least partially mediated by FGFR1

To better understand the complex network of tumor-stromal interactions in vivo, we investigated the role of osteoblast FGFR1 in promoting tumor growth by knocking down this receptor in the MC 3T3-E1 cells (Fig. 4B). We observed that at day 6, the cellularity of co-cultures of MDA PCa 118b cells and *Fgfr1*-knockdown MC 3T3-E1 cells was significantly lower ($p = 0.034$) than the cellularity of co-cultures of MDA PCa 118b cells and MC 3T3-E1 cells transfected with control siRNA but still greater than the sum of the cellularity values for the mono-cultures (Fig. 4C). This greater-than-additive effect was observed despite suppressed transcript levels of *Fgfr1* at day 6 (Fig. 4B). This observed decrease in cellularity of the co-cultures of MDA PCa 118b cells and *Fgfr1*-knockdown MC 3T3-E1 cells as compared to the controls corroborates with our previous *in vivo* study, where FGFR1 was found to be a significant mediator of the PCa cell-bone cell interaction (17).

FGFR inhibitor dovitinib decreases the cellularity of co-cultures of PDX-derived PCa cells and osteoblastic cells

Given that our previous study suggested that dovitinib, an FGFR inhibitor, mediated an antitumor effect in the in vivo MDA PCa 118b PDX model partly by blocking the PCa cell–bone cell interaction (17), we next sought to evaluate the effect of dovitinib in our 3D co-culture model. We found that while dovitinib at 1000 nM did not reduce the cellularity of MDA PCa 118b-only and MC 3T3-E1-only mono-cultures as compared to the untreated controls, dovitinib did significantly reduce the cellularity of the co-cultures by 26%, compared to the untreated controls ($p = 0.014$) (Fig. 4D). We also investigated the biochemical changes in the dovitinib-treated cells by probing for FGFR1 and *Fgfr1* transcript levels using species-specific primers. No reduction in either mouse or human transcripts was observed with increasing dovitinib concentrations (Fig. 4E). This contrasts with our previous in vivo findings that FGFR1 and *Fgfr1* transcript levels were reduced in both the tumor and bone stroma of tumor-bearing bones in dovitinib-treated animals (17). Given that FGFR blockade with dovitinib was associated with an improvement in bone quality in our previous in vivo study (17), we probed for transcript levels of a well-established marker of osteogenic activity, ALP, in dovitinib-treated MC 3T3-E1 cells. We found that ALP levels increased with increasing dovitinib concentrations (Fig. 4F). Taken together, these findings suggest that our co-culture model recapitulates two key responses to dovitinib seen in vivo, i.e., reduction in the size of the tumor microenvironment and osteogenesis.

Discussion

Increasing recognition of the dependence of cancer cells on their stromal environment has shifted the focus of researchers toward co-targeting tumor and stroma (14). For PCa, a highly microenvironment-driven cancer, few preclinical models reflect the predominantly bone-forming or osteogenic phenotype of the disease (28). Using the MDA PCa 118b PDX model (25), we previously found that use of dovitinib to interfere with the FGFR-mediated stromal-epithelial interaction in bone is a promising co-targeting strategy (17). In this follow-up study, we asked if we could develop an in vitro PCa PDX model that recapitulates the molecular mechanisms governing the PCa cell–stromal cell interaction and allows the investigator to efficiently control and manipulate the cancer cell microenvironment. Leveraging our ability to generate tumor cell–enriched PDX-derived PCa tumoroids in vitro, we co-encapsulated PCa tumoroids derived from MDA PCa 118b PDXs with MC 3T3-E1 osteoblastic cells within a 3D hydrogel. This approach yielded a striking in vivo–like re-creation of the spatial organization of tumor cells with osteoblasts in bone, maintained cell viability and proliferative capacity, and remarkably recapitulated the FGFR-mediated PCa cell–stromal cell cross-talk observed in vivo.

Alternative culture systems such as spheroid culture or basement membrane extracts have been reported as feasible systems for primary tumor cell culture ex vivo (9,11,29) but inherently provide the investigator with little control over the in vitro cancer cell microenvironment. With matrix design considerations such as biological activity and tunable properties (structural, mechanical, and composition), we previously showed that HA matrices are highly supportive of PDX culture in vitro, able to maintain long-term cell viability with retention of phenotype (21). However, HA-only hydrogels poorly support mesenchymal cell culture. To co-culture osteoblastic cells with PCa PDX cells, we specifically tailored HA hydrogels to include covalently bound integrin-binding and MMP-degradable peptidic modules, the combination of which enables precise manipulation of cell-cell and cell-matrix interactions and permitted our novel PCa cell-osteoblastic cell co-culture.

Compared to bone metastases from other cancers in which osteoblasts are few or absent, PCa bone metastases are characterized by a significant presence of osteoblasts adjacent to PCa cells as revealed by histopathological analysis (18). Indeed, when MDA PCa 118b PDXs are implanted intrafemorally, robust osteoblastic reactions mimicking characteristics of the human tumor of origin are observed, with osteoblasts present in the bone matrix near the injected tumor cells (25). Similarly, ectopic bone formation is observed around subcutaneously grown MDA PCa 118b PDX tumors (25). These observations indicate that close proximity of PCa cells to osteoblasts is a unique characteristic of PCa, and the strong osteoinductive capacity of the MDA PCa 118b PDXs underscores the well-established dependency of PCa on osteoblasts in PCa osteoblastic metastasis (18). In our model, MC 3T3-E1 cells extended cellular processes towards co-encapsulated PDX tumoroids and often enveloped the tumoroids completely, mimicking the spatial organization of MDA PCa 118b PDXs with osteoblasts in vivo. Our 3D model will thus enable future detailed examination of PCa cell–osteoblastic cell contact mechanisms and their impact on tumor progression.

Osteogenesis driven by MDA PCa 118b PDXs in vivo has been attributed to secreted paracrine factors, such as FGF9 and bone morphogenetic protein (BMP)-4, that induce osteoblast proliferation and differentiation (25,28,30). The observed increase in transcript levels of osteoblast markers (osteocalcin, bone sialoprotein, and ALP) in the co-cultured MC 3T3-E1 cells suggests that MDA PCa 118b cells in our model retained their inherent ability to induce bone formation. Additionally, the greater-than-additive effect of co-culture on cellularity and maintenance of proliferative capacity in the MDA PCa 118b cells is likely reflective of the co-stimulatory PCa cell–osteoblast relationship, which involves several growth factors, including FGFs, BMP-2, and insulin-like growth factor (17,18,25,30–32), further supporting the notion that the PCa-osteoblast cross-talk is recapitulated in our in vitro model. This is an important feature of our model as PDXs typically cannot be propagated outside the murine host.

Among the targeted therapies in preclinical and clinical development for recalcitrant advanced PCa, FGF signaling blockade has emerged as a rational therapeutic strategy (33–35). Aberrant FGF signaling regulates many mechanisms, including mitogenesis, differentiation, angiogenesis, survival, and invasiveness, and contributes to PCa progression and metastasis (25,33,34). Examples include demonstrated osteoblast proliferation in response to FGF9 produced by MDA PCa 118b cells and overexpression of FGFR1 in PCa, especially in MDA PCa 118b cells (17,25). In this study, we established that hydrogel-encapsulated MDA PCa 118b cells maintained their expression of FGFR1 and FGF9 when cultured in vitro, indicating that our hydrogel system preserves salient features of the FGF axis in these tumor cells necessary for accurate in vitro modeling of FGF signaling. Furthermore, we showed that our co-culture model strikingly recreated the intercellular cross-talk and stromal changes that occur when MDA PCa 118b cells are grown in bone. Using an orthotopic mouse model of MDA PCa 118b, we previously found that levels of stromal *Fgfr1* and *Fgf2* were increased and the level of *Fgfr4* was decreased in tumor-bearing femurs compared to the contralateral sham-injected femurs (17). While the exact molecular mechanisms governing the induction of *Fgfr1* in osteoblasts and the implications of such *Fgfr1* induction are unknown, these changes observed in vivo and in our co-culture model fit into the current paradigm describing the PCa-osteoblast relationship, in which FGFR1 and FGF2 are key mediators of the interaction and fuel both PCa and osteoblast growth in a co-stimulatory relationship (33).

To confirm that our 3D PCa PDX in vitro model permits rapid and controlled examination of specific tumor-stromal interactions within the complex in vivo tumor microenvironment, we performed a proof-of-concept experiment in which we knockdowned *Fgfr1* in the MC 3T3-E1 cells to investigate the contribution of osteoblast FGFR1 to tumor growth. The suppressed cellularity in co-cultures with *Fgfr1*-knockdown MC 3T3-E1 cells indicates that FGFR1 plays a vital role in the PCa-osteoblast interaction, as suggested in our previous study (17). *Fgfr1* manipulation did not entirely abrogate the increased cellularity in co-culture, likely because of subtotal knockdown in the MC 3T3-E1 cells and the certain presence of multiple other redundant cooperative pathways that moderate the PCa-stromal interaction (18).

In our previous study, dovitinib, a receptor tyrosine kinase inhibitor of FGFR and vascular endothelial growth factor receptor, exhibited remarkable clinical efficacy in a subset of patients with castration-resistant PCa and bone metastases (17). The antitumor effect was achieved indirectly by co-targeting the stromal compartment in bone, highlighting the therapeutic potential of disrupting the neoplastic epithelial-stromal interaction in PCa bone metastases. In contrast to the decrease in co-culture cellularity, the lack of response to dovitinib treatment in the PCa-only and osteoblastic cell–only monocultures suggests that our model reflects the tumor-stromal targeting ability of dovitinib in vivo (17). Furthermore, the increase in ALP transcript levels observed in our co-cultures suggests that FGFR signaling blockade promotes osteoblastic differentiation, which may account for the improvement of bone quality observed in vivo (17).

Given that dovitinib-induced changes in *Fgfr1* transcript levels were absent in our 3D co-culture, we propose that other cells in the tumor microenvironment contributed to the suppressive effect of dovitinib on *Fgfr1* transcript levels previously seen in vivo. Notably, the observed reduction in stromal *Fgfr1* in vivo was based on a collective measure of *Fgfr1* levels in all stromal cells in bone given that entire mouse femurs were analyzed (17). Several cell types within bone express FGFR1 (36); indeed, we previously demonstrated that the antitumor effect of dovitinib could be ascribed partially to the antiangiogenic activity of the drug, given that endothelial cells also express FGFR1 (17). Current work in our laboratories seeks to increase the cellular complexity of our 3D hydrogel co-culture models to include elements of the vasculature and innate immune system. Although the current model is limited by the use of mouse-derived osteoblastic cells to model the PCa-osteoblast interaction, studies are under way to develop a human-only system. Our modular system will facilitate mechanistic studies that systematically dissect the complex effect of dovitinib in vivo by investigating the role of different stromal cell types on overall drug efficacy.

In conclusion, using a bottom-up approach with the capacity for engineered complexity, we established an in vitro auxiliary to an established murine-host PCa PDX model. Our 3D modular hydrogel system enables rapid, controlled mechanistic studies aimed at deconvoluting complex in vivo tumor-stroma interactions. This study demonstrates remarkable consistency in tumor architecture, phenotype, and tumor-stromal signaling between the patient’s tumor, the corresponding PDX model, and our in vitro PDX model. Future studies may benefit from this translational approach of employing high fidelity PDX cells in controlled 3D *in vitro* systems to support rapid interrogation of complex *in vivo* and clinical findings.

Supplementary Material

Refer to Web version on PubMed Central for supplementary material.

Acknowledgments

We thank Dr. Xinqiao Jia from the University of Delaware for sharing her expertise in HA hydrogels. This research was supported in part by National Institutes of Health grants P01 CA098912, R01 CA180279, and Prostate SPORE grant 5P50 CA140388; the Cancer Prevention & Research Institute of Texas grant RP11055; and the David H. Koch Center for Applied Research in Genitourinary Cancers at The University of Texas MD Anderson Cancer

Center. E.L.S.F. acknowledges funding support from the National University of Singapore-Overseas Graduate Scholarship.

References

1. Hutchinson L, Kirk R. High drug attrition rates-where are we going wrong? Nat Rev Clin Oncol. 2011; 8(4):189–190. [PubMed: 21448176]
2. Begley CG, Ellis LM. Drug development: Raise standards for preclinical cancer research. Nature. 2012; 483(7391):531–533. [PubMed: 22460880]
3. Zhao X, Liu Z, Yu L, Zhang Y, Baxter P, Voicu H, et al. Global gene expression profiling confirms the molecular fidelity of primary tumor-based orthotopic xenograft mouse models of medulloblastoma. Neuro Oncol. 2012; 14(5):574–583. [PubMed: 22459127]
4. DeRose YS, Wang G, Lin YC, Bernard PS, Buys SS, Ebbert MT, et al. Tumor grafts derived from women with breast cancer authentically reflect tumor pathology, growth, metastasis and disease outcomes. Nat Med. 2011; 17(11):1514–1520. [PubMed: 22019887]
5. Loukopoulos P, Kanetaka K, Takamura M, Shibata T, Sakamoto M, Hirohashi S. Orthotopic transplantation models of pancreatic adenocarcinoma derived from cell lines and primary tumors and displaying varying metastatic activity. Pancreas. 2004; 29(3):193–203. [PubMed: 15367885]
6. Williams SA, Anderson WC, Santaguida MT, Dylla SJ. Patient-derived xenografts, the cancer stem cell paradigm, and cancer pathobiology in the 21st century. Lab Invest. 2013; 93(9):970–982. [PubMed: 23917877]
7. Peng S, Creighton CJ, Zhang Y, Sen B, Mazumdar T, Myers JN, et al. Tumor grafts derived from patients with head and neck squamous carcinoma authentically maintain the molecular and histologic characteristics of human cancers. J Transl Med. 2013; 11:198. [PubMed: 23981300]
8. Siolas D, Hannon GJ. Patient-derived tumor xenografts: transforming clinical samples into mouse models. Cancer Research. 2013; 73(17):5315–5319. [PubMed: 23733750]
9. Gao D, Vela I, Sboner A, Iaquinta PJ, Karthaus WR, Gopalan A, et al. Organoid cultures derived from patients with advanced prostate cancer. Cell. 2014; 159(1):176–187. [PubMed: 25201530]
10. Sueblinvong T, Ghebre R, Iizuka Y, Pambuccian SE, Isaksson Vogel R, Skubitz AP, et al. Establishment, characterization and downstream application of primary ovarian cancer cells derived from solid tumors. PLoS One. 2012; 7(11):e50519. [PubMed: 23226302]
11. Kondo J, Endo H, Okuyama H, Ishikawa O, Iishi H, Tsujii M, et al. Retaining cell-cell contact enables preparation and culture of spheroids composed of pure primary cancer cells from colorectal cancer. Proc Natl Acad Sci U S A. 2011; 108(15):6235–6240. [PubMed: 21444794]
12. Weiswald LB, Richon S, Validire P, Briffod M, Lai-Kuen R, Cordelieres FP, et al. Newly characterised ex vivo colospheres as a three-dimensional colon cancer cell model of tumour aggressiveness. Br J Cancer. 2009; 101(3):473–482. [PubMed: 19603013]
13. Dayyani F, Gallick GE, Logothetis CJ, Corn PG. Novel therapies for metastatic castrate-resistant prostate cancer. J Natl Cancer Inst. 2011; 103(22):1665–1675. [PubMed: 21917607]
14. Sluka P, Davis ID. Cell mates: paracrine and stromal targets for prostate cancer therapy. Nat Rev Urol. 2013; 10(8):441–451. [PubMed: 23857181]
15. Sung SY, Hsieh CL, Law A, Zhau HE, Pathak S, Multani AS, et al. Coevolution of prostate cancer and bone stroma in three-dimensional coculture: implications for cancer growth and metastasis. Cancer Research. 2008; 68(23):9996–10003. [PubMed: 19047182]
16. Li YM, Sikes RA, Malaeb BS, Yeung F, Law A, Graham SE, et al. Osteoblasts can stimulate prostate cancer growth and transcriptionally down-regulate PSA expression in cell line models. Urologic Oncology-Seminars and Original Investigations. 2011; 29(6):802–808.
17. Wan X, Corn PG, Yang J, Palanisamy N, Starbuck MW, Efstathiou E, et al. Prostate cancer cell-stromal cell crosstalk via FGFR1 mediates antitumor activity of dovitinib in bone metastases. Sci Transl Med. 2014; 6(252):252ra122.
18. Logothetis CJ, Lin SH. Osteoblasts in prostate cancer metastasis to bone. Nat Rev Cancer. 2005; 5(1):21–28. [PubMed: 15630412]

19. Gurski LA, Jha AK, Zhang C, Jia X, Farach-Carson MC. Hyaluronic acid-based hydrogels as 3D matrices for in vitro evaluation of chemotherapeutic drugs using poorly adherent prostate cancer cells. Biomaterials. 2009; 30(30):6076–6085. [PubMed: 19695694]
20. Xu X, Gurski LA, Zhang C, Harrington DA, Farach-Carson MC, Jia XQ. Recreating the tumor microenvironment in a bilayer, hyaluronic acid hydrogel construct for the growth of prostate cancer spheroids. Biomaterials. 2012; 33(35):9049–9060. [PubMed: 22999468]
21. Fong EL, Martinez M, Yang J, Mikos AG, Navone NM, Harrington DA, et al. Hydrogel-based 3D model of patient-derived prostate xenograft tumors suitable for drug screening. Mol Pharm. 2014; 11(7):2040–2050. [PubMed: 24779589]
22. Lei Y, Gojgini S, Lam J, Segura T. The spreading, migration and proliferation of mouse mesenchymal stem cells cultured inside hyaluronic acid hydrogels. Biomaterials. 2011; 32(1):39–47. [PubMed: 20933268]
23. Lutolf MP, Lauer-Fields JL, Schmoekel HG, Metters AT, Weber FE, Fields GB, et al. Synthetic matrix metalloproteinase-sensitive hydrogels for the conduction of tissue regeneration: engineering cell-invasion characteristics. Proc Natl Acad Sci U S A. 2003; 100(9):5413–5418. [PubMed: 12686696]
24. Kim J, Park Y, Tae G, Lee KB, Hwang SJ, Kim IS, et al. Synthesis and characterization of matrix metalloprotease sensitive-low molecular weight hyaluronic acid based hydrogels. J Mater Sci Mater Med. 2008; 19(11):3311–3318. [PubMed: 18496734]
25. Li ZG, Mathew P, Yang J, Starbuck MW, Zurita AJ, Liu J, et al. Androgen receptor-negative human prostate cancer cells induce osteogenesis in mice through FGF9-mediated mechanisms. J Clin Invest. 2008; 118(8):2697–2710. [PubMed: 18618013]
26. Shu XZ, Liu YC, Luo Y, Roberts MC, Prestwich GD. Disulfide cross-linked hyaluronan hydrogels. Biomacromolecules. 2002; 3(6):1304–1311. [PubMed: 12425669]
27. Zhang X, Xu B, Puperi DS, Yonezawa AL, Wu Y, Tseng H, et al. Integrating valve-inspired design features into poly(ethylene glycol) hydrogel scaffolds for heart valve tissue engineering. Acta Biomater. 2015; 14:11–21. [PubMed: 25433168]
28. Lee YC, Cheng CJ, Bilen MA, Lu JF, Satcher RL, Yu-Lee LY, et al. BMP4 promotes prostate tumor growth in bone through osteogenesis. Cancer Research. 2011; 71(15):5194–5203. [PubMed: 21670081]
29. Weiswald LB, Richon S, Massonnet G, Guinebretiere JM, Vacher S, Laurendeau I, et al. A short-term colorectal cancer sphere culture as a relevant tool for human cancer biology investigation. Br J Cancer. 2013; 108(8):1720–1731. [PubMed: 23538387]
30. Yang J, Fizazi K, Peleg S, Sikes CR, Raymond AK, Jamal N, et al. Prostate cancer cells induce osteoblast differentiation through a Cbfa1-dependent pathway. Cancer Research. 2001; 61(14): 5652–5659. [PubMed: 11454720]
31. Fizazi K, Yang J, Peleg S, Sikes CR, Kreimann EL, Daliani D, et al. Prostate cancer cells-osteoblast interaction shifts expression of growth/survival-related genes in prostate cancer and reduces expression of osteoprotegerin in osteoblasts. Clin Cancer Res. 2003; 9(7):2587–2597. [PubMed: 12855635]
32. Lu Y, Zhang J, Dai J, Dehne LA, Mizokami A, Yao Z, et al. Osteoblasts induce prostate cancer proliferation and PSA expression through interleukin-6-mediated activation of the androgen receptor. Clin Exp Metastasis. 2004; 21(5):399–408. [PubMed: 15672864]
33. Corn PG, Wang F, McKeehan WL, Navone N. Targeting fibroblast growth factor pathways in prostate cancer. Clin Cancer Res. 2013; 19(21):5856–5866. [PubMed: 24052019]
34. Valta MP, Tuomela J, Bjartell A, Valve E, Vaananen HK, Harkonen P. FGF-8 is involved in bone metastasis of prostate cancer. Int J Cancer. 2008; 123(1):22–31. [PubMed: 18386787]
35. Sahadevan K, Darby S, Leung HY, Mathers ME, Robson CN, Gnanapragasam VJ. Selective over-expression of fibroblast growth factor receptors 1 and 4 in clinical prostate cancer. J Pathol. 2007; 213(1):82–90. [PubMed: 17607666]
36. van Hinsbergh VW, Rabelink TJ. FGFR1 and the bloodline of the vasculature. Arterioscler Thromb Vasc Biol. 2005; 25(5):883–886. [PubMed: 15863718]

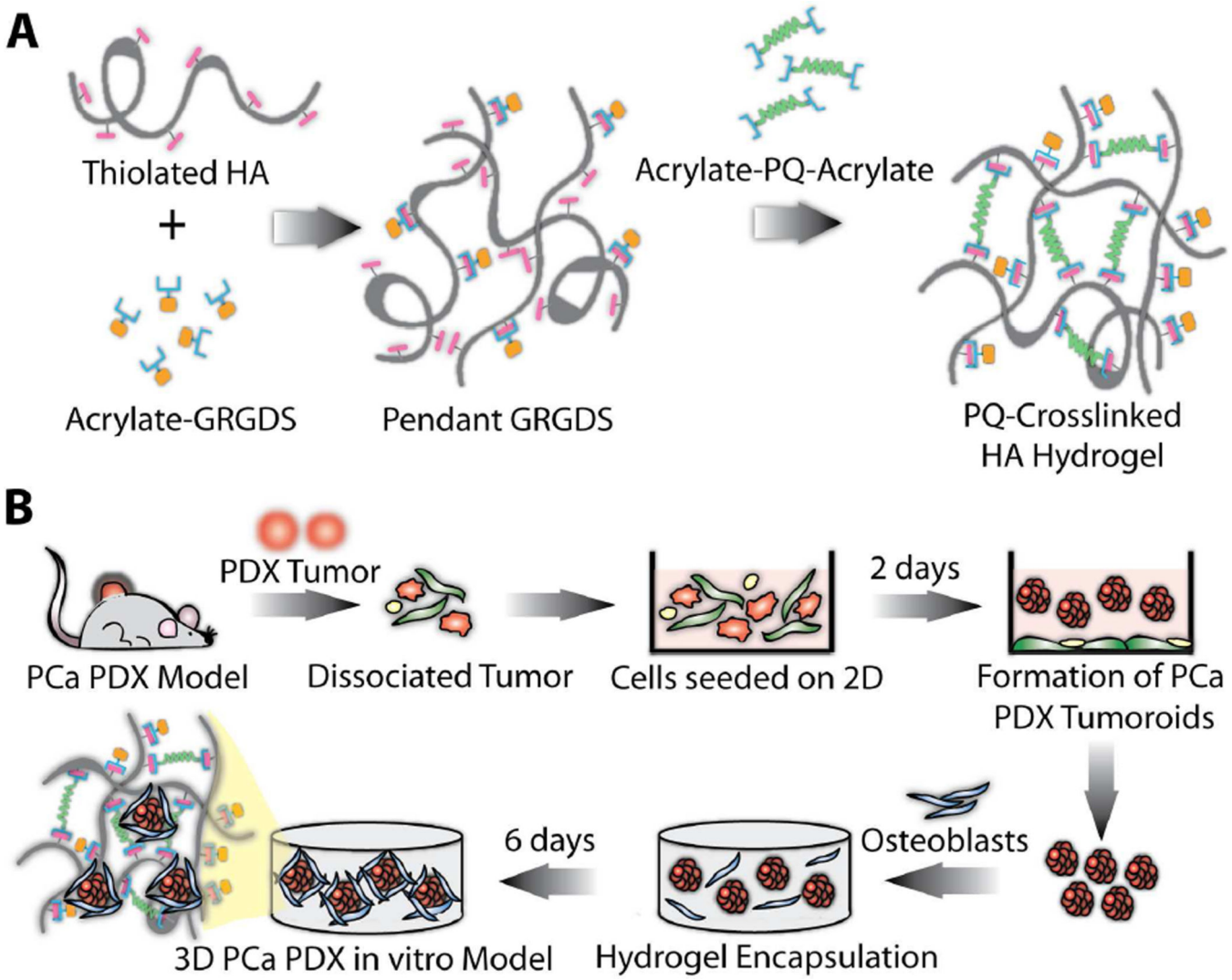

Fig. 1.

Schematic of 3D hydrogel system and co-culture fabrication. (**A**) The hydrogel system comprises thiolated HA and acrylate-functionalized peptides, GRGDS (integrin-binding) and PQ (MMP-sensitive). (**B**) PDX tissue harvested from the animal is digested and then plated in 6-well plates to allow formation of tumor aggregates. Resulting tumoroids are collected and then co-encapsulated with osteoblastic cells.

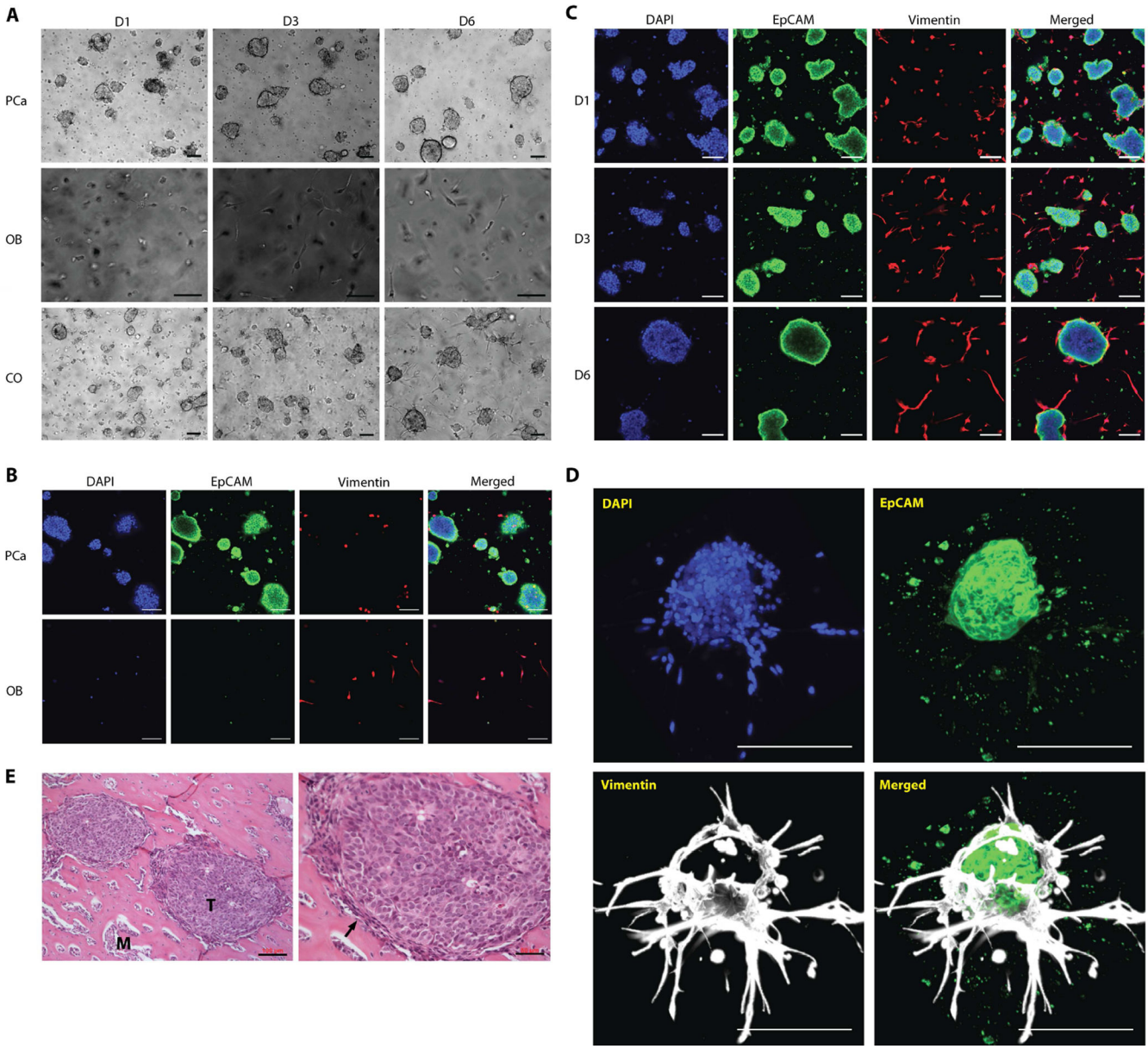

Fig. 2.

PCa cell–osteoblastic cell organization in co-culture. (**A**) Bright-field images of MDA PCa 118b-only cultures (PCa), MC 3T3-E1-only cultures (OB), and co-cultures (CO) obtained on day 1 (D1), day 3 (D3), and day 6 (D6). Scale bars = 100 μm. (**B and C**) EpCAM and vimentin expression were used to show the EpCAM-positive (green) tumor cells and the vimentin-positive (red) osteoblastic cells in (B) PCa-only and OB-only mono-cultures and (C) co-cultures at D6. Physical association of the osteoblastic cells with the tumor cells was most evident at D6. Scale bars = 100 μm. (**D**) 3D volume rendering of an osteoblast-wrapped PCa tumoroid in co-culture. Scale bar = 100 μm. (**E**) Hematoxylin-eosin-stained sections of intrafemorally grown MDA PCa 118b PDX. T = tumor, M = bone matrix; black arrow indicates osteoblasts. Scale bar left image = 100 μm; scale bar right image = 50 μm.

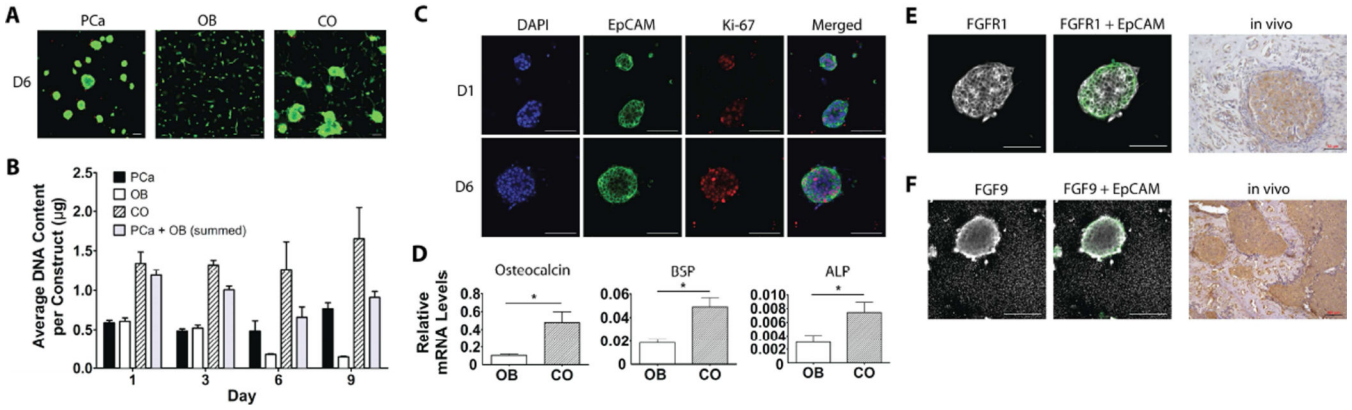

Fig. 3.

Growth profile and preservation of in vivo tumor phenotype in co-culture. (**A**) MDA PCa 118b-only cultures (PCa), MC 3T3-E1-only cultures (OB), and co-cultures (CO) processed under the LIVE/DEAD viability assay, in which green staining indicates viable cells and red staining indicates nonviable cells. Cells in mono- or co-cultures were viable at day 6 (D6). Scale bars = 100 μm. (**B**) DNA content of actual co-cultures (CO) was consistently higher than the sum of DNA content of mono-cultures (PCa + OB). N = 4. (**C**) MDA PCa 118b cells were positive for Ki-67 at all measured time points in culture. Shown are immunostained co-culture constructs at D1 and D6. (**D**) Transcripts encoding osteocalcin, bone sialoprotein (BSP), and alkaline phosphatase (ALP) relative to GAPDH in MC 3T3-E1 cells (D6) were higher in co-culture (CO) than in mono-culture (OB). N = 4. *$p < 0.05$. (**E and F**) MDA PCa 118b cells retained expression of (E) FGFR1 and (F) FGF9 in the 3D co-culture model (D6). Constructs were co-stained for EpCAM (green) to identify the tumor cells in co-culture. Scale bars = 100 μm. MDA PCa 118b cells grown in bone (right-most panel) express (E) FGFR1 (scale bar = 50 μm) and (F) FGF9 (scale bar = 100 μm).

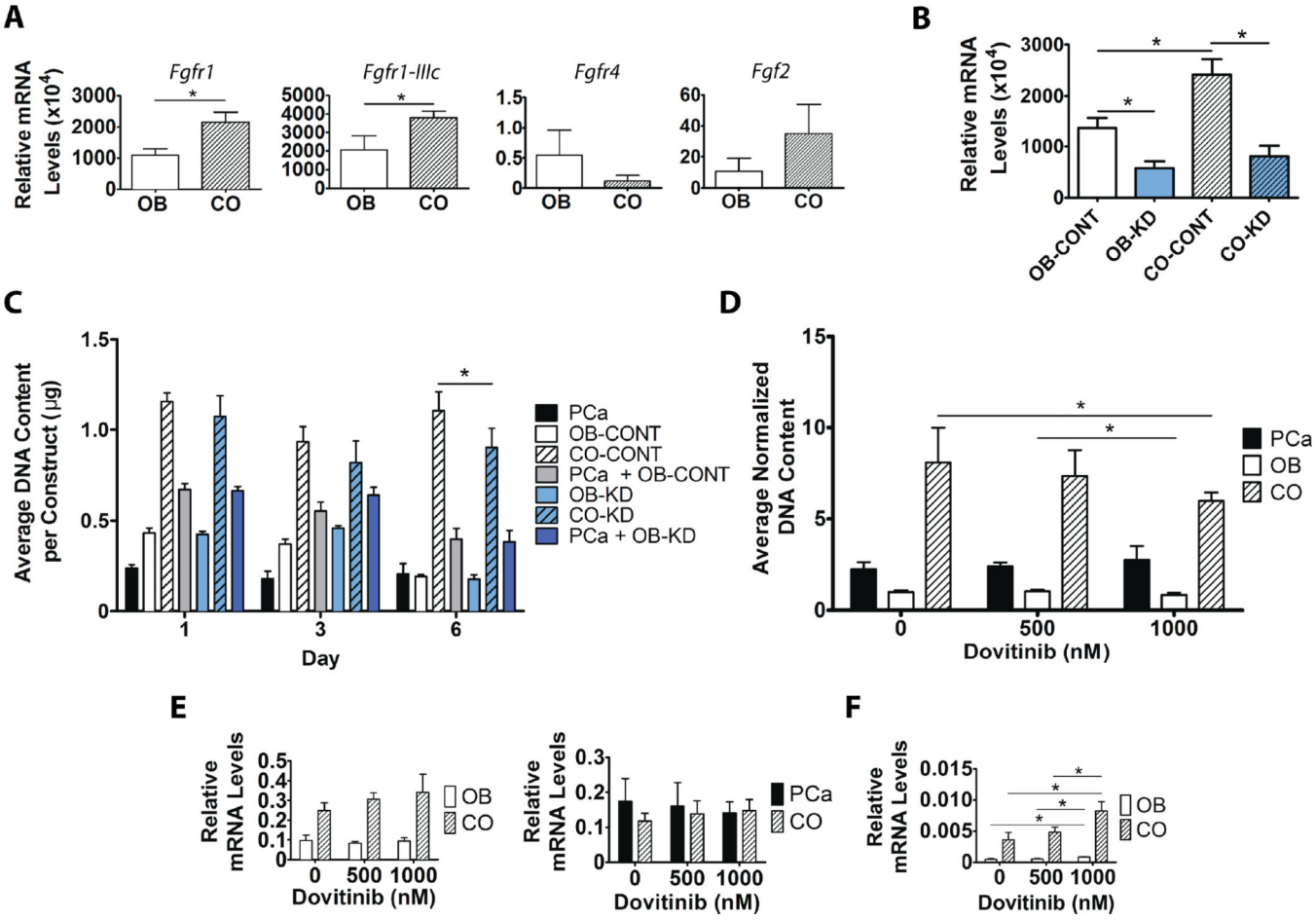

Fig. 4.

Manipulation of FGFR-mediated biochemical cross-talk between PCa and osteoblastic cells in co-culture. (**A**) Transcripts encoding FGF signaling components in MC 3T3-E1 cells, relative to GAPDH. N = 4. Differences in levels of *Fgfr1, Fgfr1-IIIc*, *Fgfr4*, and *Fgf2* transcripts at day 6 (D6) were observed between MC 3T3-E1 cells in mono-cultures (OB) and MC 3T3-E1 cells co-cultured (CO) with MDA PCa 118b cells. *p < 0.05. (**B**) Transcripts encoding *Fgfr1* in the MC 3T3-E1 cells (relative to GAPDH) under various conditions. N = 3. *p < 0.05. *Fgfr1*-knockdown MC 3T3-E1 cells (OB-KD) and scrambled controls (OB-CONT) were co-cultured with MDA PCa 118b cells (CO-KD and CO-CONT, respectively). (**C**) DNA contents of the cultures in (B) and the other cultures indicated in the figure were measured over time. N = 4. Average DNA content of CO-KD cultures was lower than that of the CO-CONT cultures at D6. Average DNA content of CO-KD cultures was higher than the sum of the DNA content of mono-cultures (PCa + OB-KD), similar to what was observed with the CO-CONT cultures (compared to summed PCa + OB-CONT values), despite suppressed levels of *Fgfr1* at D6, as shown in (B). (**D**) Normalized DNA content of dovitinib-treated mono-cultures (PCa and OB) and co-cultures (CO). *p < 0.05. Results shown are a combination of two identically performed studies. N = 8. (**E**) Transcripts encoding human FGFR1 and mouse *Fgfr1* (relative to GAPDH) in co-cultures in the presence of increasing dovitinib concentration. N = 3. (**F**) Transcripts encoding mouse

ALP (relative to GAPDH) in mono-cultures and co-cultures in the presence of increasing dovitinib concentrations. N = 3. *$p < 0.05$. Transcript levels of ALP increased with increasing dovitinib concentrations.